Multiplicity Fluctuation and Single-Particle Spectrum in Two-Jet Events in e^+e^- Annihilation

T. T. Chou
Department of Physics, University of Georgia, Athens, Georgia 30602

and

Chen Ning Yang
Institute for Theoretical Physics, State University of New York, Stony Brook, New York 11794
(Received 8 May 1985)

Recent ideas in the geometrical model of multiparticle production in hadron-hadron collisions are applied to two-jet events in e^+e^- annihilation. A coherent picture emerges which is compared with experimental data. A number of predictions are made, including the prediction that Koba-Nielsen-Olesen scaling does not obtain for such events. The relationship with QCD models remains unexplored.

PACS numbers: 12.40.Ee, 12.40.Pp

Two recent ideas in the geometrical model of multiparticle production in hadron-hadron collisions have led to a good approximate picture for the forward-backward asymmetry distribution and the single-particle spectrum. These ideas are (i) that[1] at a given impact parameter b the forward and backward hemispheres have charged-particle multiplicities n_F and n_B distributed in a *stochastic* manner [i.e., not according to Koba-Nielsen-Olesen (KNO) scaling] and (ii) that[2,3] in this stochastic process the energy partition on each side is governed (mainly) by a parameter called partition temperature. In the present paper we apply these ideas to hadron production in high-energy e^+e^- annihilation experiments, taking the thrust axis or the sphericity axis[4] as the analog of the incoming hadron direction in $p\bar{p}$ collision. We ignore three- or more-jet events.

No KNO scaling in e^+e^- annihilation.—In e^+e^- annihilation, the total angular momentum of the virtual boson is 0 or 1 (which is consistent with the experimental angular distribution of the jet axis at the DESY e^+e^- storage ring PETRA[5]). This is in sharp contrast to the case of $p\bar{p}$ collider experiments for which it was emphasized in Refs. 1–3 that the angular momentum ranges from 0 to $\sim 2000\hbar$. In the latter case, the KNO fluctuation is interpreted as due to this wide range of angular momentum. It follows that for the former case, where there is (essentially) no fluctuation of angular momentum, there should be no KNO scaling. This conclusion is the *opposite of the universally accepted idea* that KNO scaling is observed in e^+e^- annihilation as well as in hadron-hadron collisions.

Poisson-type multiplicity distribution in e^+e^- annihilation.—Consistent with the ideas explored in Refs. 1–3, we conclude that the multiplicity distribution in e^+e^- annihilation is a Poisson distribution (i.e., stochastic.)

Does this conclusion contradict existing experimental data? We believe not. In fact, Fig. 2 of Ref. 5 indicates to us that the TASSO Collaboration results at $W=14$, 22, and 34 GeV support our conclusion, although Ref. 5 seems to lean toward the opposite conclusion. (We call attention to the fact that for $W=34$ GeV, the curve exhibits an extensive region of positive curvature on the low-multiplicity side of the peak, in sharp contrast to the $p\bar{p}$ case.) The crucial tests will, of course, come with future Stanford Linear Collider (SLC) and CERN LEP two-jet experiments.

Furthermore, if one takes an ingenuous attitude, one would find that the multiplicity distributions for e^+e^- and $p\bar{p}$ collisions plotted in Fig. 8 of Ref. 5 exhibit a striking qualitative difference: The former is simple and the latter complex. We believe that this difference reflects the fact that the former is a pure Poisson distribution and therefore simple, while the latter is a complex superposition of many Poisson distributions.

Product of Poisson distributions on each side.—Consistent with the above picture and the results of Ref. 1, for e^+e^- annihilation the distributions with respect to the forward and backward[6] multiplicities n_F and n_B should be a product of two Poisson distributions,

$$P(n_F,n_B)=\left[\exp\left(-\frac{\bar{n}}{4}\right)\frac{(\bar{n}/4)^{n_F/2}}{(n_F/2)!}\right]\left[\exp\left(-\frac{\bar{n}}{4}\right)\frac{(\bar{n}/4)^{n_B/2}}{(n_B/2)!}\right], \tag{1}$$

where $\bar{n}/2$ is the average charge multiplicity on each side. The factors 2 in $n_F/2$ and $n_B/2$ derive[1] from the fact that pairs of particles of opposite charge are emitted.

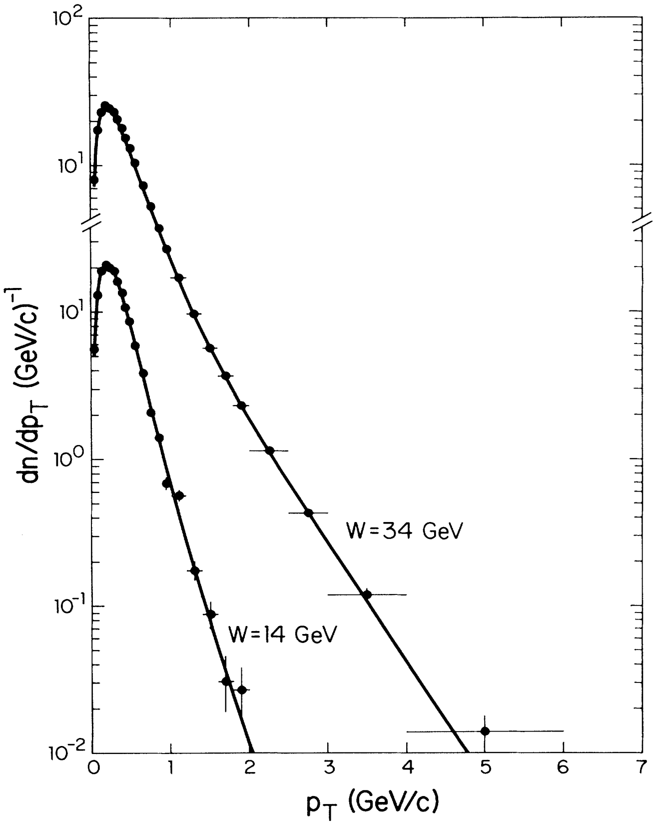

FIG. 1. The calculated dn/dp_T distributions for e^+e^- annihilation at $W=14$ and 34 GeV. The experimental data points are taken from Ref. 5.

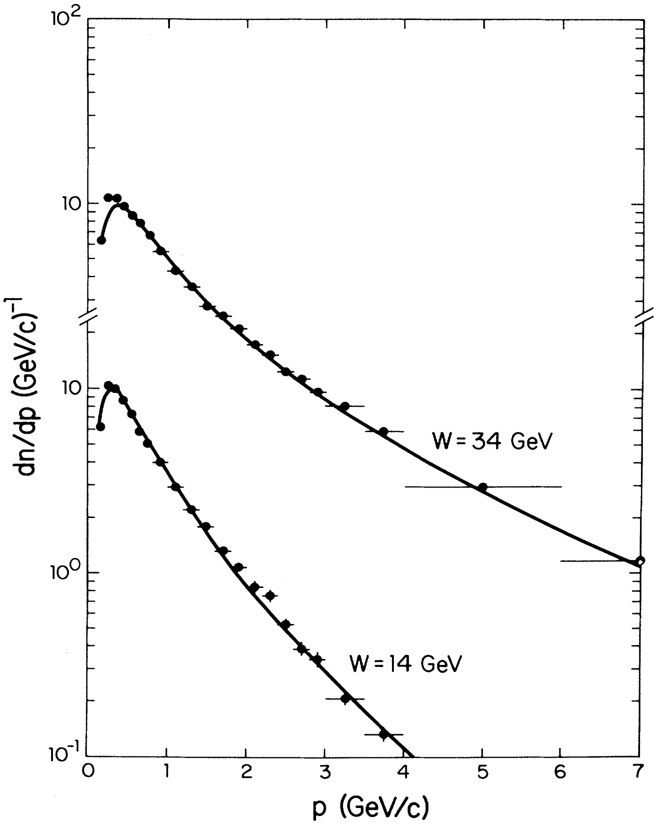

FIG. 2. The calculated charged-particle momentum spectrum dn/dp for e^+e^- annihilation at $W=14$ and 34 GeV. The experimental data points are taken from Ref. 5.

Notice that with (1), at a fixed total $n=n_F+n_B$, the distribution with respect to n_F is proportional[1] to a binomial:

$$P(n_F,n_B)=(\text{const})C^{n/2}_{n_F/2}. \tag{2}$$

Approximate zero net charge on each side.—The picture described above implies

$$(\text{net charge in forward direction})/\bar{n}\to 0 \quad \text{as } \bar{n}\to\infty. \tag{3}$$

In fact we believe a stronger statement:

$$(\text{net charge in forward direction})/\sqrt{\bar{n}}\to 0 \quad \text{as } \bar{n}\to\infty. \tag{3a}$$

These can be simply tested experimentally both in existing PETRA data and in future SLC and LEP experiments.

Single-particle momentum distribution in e^+e^- collision.—In the picture described above, e^+e^- collision is similar to hadron-hadron collision at impact parameter $\simeq 0$. Using the same argument as in Refs. 2 and 3, one arrives at the following one-particle momentum distribution:

$$dn=dn^{\text{ch}}=(d^3p/E)G(p_T)\exp(-E/T_p), \tag{4}$$

where $G(p_T)$ is a transverse-momentum cutoff factor, previously written as $Kg(p_T)$.

To test whether (4) gives generally a good approximation to the single-particle spectrum, we made simple choices of the values of $G(p_T)$ and T, computed from (4) the distributions dn/dp_T and dn/dp, and compared the results with TASSO data[5] on these distributions. No "best-fit" procedures were attempted. The results are presented in Figs. 1 and 2, for which the following choices were made:

$$T_p=1.6\text{ GeV},\quad 4\pi G(p_T)=70[3\exp(-6.2p_T)-2\exp(-13p_T)]\exp(0.8p_T^2)\ (\text{GeV}/c)^{-2} \quad (\text{for } p_T<3.5\text{ GeV}/c)\text{ for } W=14\text{ GeV};$$

$$T_p=3.3\text{ GeV},\quad 4\pi G(p_T)=(100e^{-4.5p_T}+3.5e^{-1.7p_T})\ (\text{GeV}/c)^{-2}\text{ for } W=34\text{ GeV}. \tag{5}$$

TABLE I. Qualitative differences between $p\bar{p}$ or pp collision and e^+e^- annihilation.

$p\bar{p}$ or pp collision	e^+e^- annihilation
Wide range of angular momentum	Angular momentum = 0,1
Wide range of T_p	Single T_p
KNO scaling	No KNO scaling

Discussion.—(a) We summarize the qualitative differences of pp and $p\bar{p}$ collisions from e^+e^- annihilation in Table I, each at a fixed high energy.

(b) In Ref. 2 and in the above discussion we have taken the transverse cutoff factor $G(p_T)$ to be independent of $p_{\parallel}$. That is too simple an assumption to give an exact description of the data. For example, in Ref. 5, Figs. 34(a) and 34(b), the average of p_T has been measured to depend appreciably on $p_{\parallel}$. Also there is clearly a positively charged–negatively charged particles correlation which is not taken into consideration in (4), as already emphasized elsewhere.[2,3] What Figs. 1 and 2 above demonstrate is that (4) is a good *first approximation* to the single-particle spectrum.

(c) In (4) the factor $\exp(-E/T_p)$ is effectively an "energy cutoff" factor. One may ask whether another energy cutoff factor, such as $\exp(-\beta E^2)$, could equally fit the data. To analyze this question, we rewrite (4) as

$$dn = (d^3p/E)G(p_T)L(E), \tag{6}$$

where L is the energy cutoff factor. For $p >> \langle p_T\rangle$ and $p >> m_\pi$, one obtains

$$p\,dn/dp \simeq 4\pi L(p)\int_0^\infty G(p_T)p_T\,dp_T. \tag{7}$$

The integral is a numerical constant and (7) can be used to solve for $L(p)$ from the experimental data on dn/dp. The result confirms very well the exponential relationship $L(E) = \exp(-E/T_p)$.

(d) One can compare (i) the picture above for e^+e^- annihilation at total energy W with (ii) the picture for $p\bar{p}$ collision with the same[2,3] central energy $2E_0h = W$ and at impact parameter $b \simeq 0$. Both cases have the same total angular momentum $\simeq 0$. Would they have the same average multiplicity $\langle n\rangle$? In Fig. 3 we plot $\langle n\rangle$ against $W = 2E_0h$ for both cases and find that $\langle n\rangle$ is much larger for $p\bar{p}$ collisions than for e^+e^- collisions. We speculate that the reason for this may lie in the following. In $p\bar{p}$ collisions, for the case $b \simeq 0$, the quark-gluon system on each side will have to go through a quark-gluon system moving in the opposite direction at high speeds. In contrast, in e^+e^- annihilation, the quark and antiquark produced merely have to struggle against the confining static plasma that surrounds them.

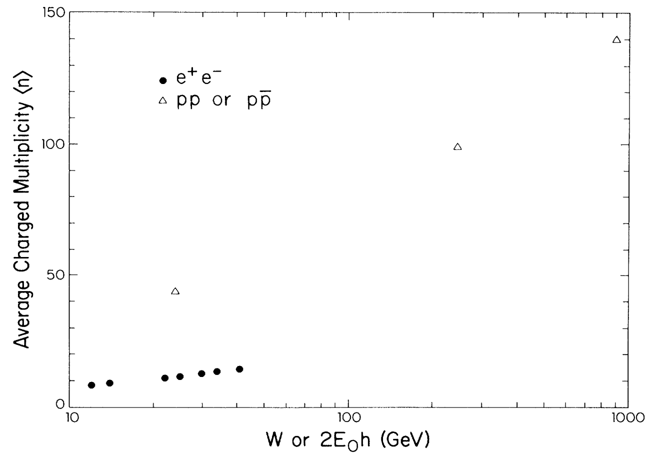

FIG. 3. Plot of average charge multiplicity $\langle n\rangle$ vs total energy W for e^+e^- annihilation or central energy $2E_0h$ for $p\bar{p}$ collision at approximately zero impact parameter. The average multiplicities for $p\bar{p}$ collisions are crude estimates subject to large uncertainties.

Comparisons of the average multiplicity in e^+e^- annihilation and in $p\bar{p}$ or pp collisions have been made before.[7,8] In these earlier comparisons no consideration was given to the spread of angular momentum in pp and $p\bar{p}$ collisions which is absent in e^+e^- collisions.

This work is supported in part by the U.S. Department of Energy under Grant No. DE-FG09-84ER40160, and by the National Science Foundation under Grant No. PHY 81-09110 A01.

[1]T. T. Chou and Chen Ning Yang, Phys. Lett. **135B**, 175 (1984).

[2]T. T. Chou, Chen Ning Yang, and E. Yen, Phys. Rev. Lett. **54**, 510 (1985).

[3]T. T. Chou and Chen Ning Yang, Phys. Rev. D **32**, 1692 (1985).

[4]J. D. Bjorken and S. J. Brodsky, Phys. Rev. D **1**, 1416 (1970); S. Brandt *et al.*, Phys. Lett. **12**, 57 (1964); E. Farhi, Phys. Rev. Lett. **39**, 1587 (1977).

[5]M. Althoff *et al.*, Z. Phys. C **22**, 307 (1984).

[6]We define forward and backward as referring to the jet axis or sphericity axis.

[7]M. Basile *et al.*, Phys. Lett. **95B**, 311 (1980).

[8]See Fig. 5 of Ref. 5.